Catalysis Letters 14 (1992) 251–261

Thermal desorption in the pressure gap and at high pressure using a Micro Knudsen Effusion Cell

Keith V. Guinn and Richard K. Herz

Chemical Engineering Group, Department of Applied Mathematics and Engineering Science, University of California, San Diego, La Jolla, CA 92093-0310, USA

Received 30 October 1991; accepted 8 May 1992

A new method and apparatus are described for performing thermal desorption at relatively high adsorbate pressure over single crystals and over porous adsorbents and catalysts. The apparatus, a Micro Knudsen Effusion Cell, encloses a sample in a small chamber or cell and allows only a limited pumping speed from the cell. Adsorbate pressures from ultrahigh vacuum to industrial reaction pressures are attainable depending on the ratio of surface area to pumping speed.

Keywords: Thermal desorption; TPD; pressure gap; Micro Knudsen Effusion Cell

1. Introduction

In this paper, we describe a new method and apparatus for performing thermal desorption. The thermal desorption or temperature programmed desorption (TPD technique involves the measurement of the net desorption rate of an adsorbate as the adsorbent temperature is increased [1–4]. The new apparatus, which we refer to as a Micro Knudsen Effusion Cell (μKEC), is capable of determining kinetic and thermodynamic parameters for adsorption and desorption over a wide range of temperatures and adsorbate pressure [5,6]. Using the μKEC, thermal desorption can be performed in the "pressure gap" region (10^{-5}–10^{1} Pa) [7,8] on both low-surface-area single crystals and high-surface-area porous adsorbents and catalysts. Thermal desorption in the pressure gap provides an opportunity to verify single crystal adsorption–desorption correlations developed at UHV adsorbate pressures ($< 10^{-5}$ Pa) and allows a direct comparison of the adsorption–desorption behavior of single crystals and porous catalysts under similar temperature and adsorbate pressure conditions. Also, thermal desorption studies at "process" conditions (10^{2}–10^{6} Pa) can be performed on high-surface-area porous catalysts using the μKEC.

Ungarish and Schmidt [9] have considered the possibility of performing thermal desorption at relatively high pressures and have analyzed the governing equations as a function of adsorbate background pressure. Ungarish and Schmidt concluded that thermal desorption "... at high pressures requires either a large area sample or the ability to measure very small pressure changes in the presence of large background pressures." Our analysis of the equations describing thermal desorption indicates that use of a high ratio of sample surface area to pumping speed is a practical method of establishing relatively high adsorbate pressures. The μKEC experiment is able to establish "high" adsorbate pressures by placing the sample in a small volume and allowing only a limited pumping speed from this volume.

2. Model

A model of the thermal desorption experiment is presented in order to illustrate the relationships between experimental parameters, such as heating rate and pumping speed, and the experimental variables surface coverage, temperature and pressure. In the specified absence of spatial gradients, surface and gas-phase balances are given by

$$\frac{\mathrm{d}\theta}{\mathrm{d}t} = r_{\mathrm{ads}} - r_{\mathrm{des}}, \tag{1}$$

$$\frac{\mathrm{d}c'}{\mathrm{d}t} = r_{\mathrm{des}} - r_{\mathrm{ads}} - r_{\mathrm{eff}}, \tag{2}$$

where θ is the fractional adsorbate surface density, c' is the dimensionless adsorbate gas concentration, and t is time. The terms r_{des} and r_{ads} are rates of desorption from and adsorption onto the sample. The term r_{eff} is the rate of effusion of adsorbate from the μKEC.

First-order Langmuir adsorption over a uniform surface with no lateral interactions and non-activated adsorption is specified here. Although real surfaces exhibit more complex behavior, this simple case is considered here in order to provide for analytical solution of the equations and for comparison with results in the literature obtained by others [10,11]. For the specified adsorption model, the desorption and adsorption rates can be expressed as

$$r_{\mathrm{des}} = \frac{\theta}{\tau_{\mathrm{des}}} = \nu_0 \exp\left(\frac{-E_{\mathrm{d}}}{RT}\right)\theta, \tag{3}$$

$$r_{\mathrm{ads}} = \frac{c'}{\tau_{\mathrm{ads}}} = \frac{S(\theta, T)FA}{V}c' = \frac{S_0 FA}{V}c'(1-\theta), \tag{4}$$

Table 1

Dimensional variables and parameters:			
A	surface area of sample	cm^2	
A_0	cross section area of equivalent ideal orifice	cm^2	
c	gas adsorbate concentration	mol/cm^3	
E_d	desorption activation energy	kJ/mol	
F	average molecular velocity	cm/s	$(RT/2\pi M)^{1/2}$
$k_d(\theta, T)$	desorption rate constant	1/s	
M	adsorbate molecular weight	kg/mol	
P	adsorbate pressure	Pa	c/RT
R	universal gas constant	kJ/mol K	
r_{ads}	scaled rate of adsorption onto the sample	1/s	c'/τ_{ads}
r_{des}	scaled rate of desorption from sample	1/s	θ/τ_{des}
r_{eff}	scaled rate of effusion from μKEC	1/s	c'/τ_{eff}
t	time	s	
T	sample and cell temperature	K	$T_i + \beta t$
V	μKEC internal volume	cm^3	
β	sample and cell temperature ramping rate	K/s	
ν_0	desorption rate pre-experimental	1/s	
σ_0	sample site density	mol/cm^2	
σ	surface adsorbate density	mol/cm^2	
τ_{ads}	characteristic time for adsorption onto the sample	s	$V/S(\theta, T)FA$
τ_{des}	characteristic time for desorption from the sample	s	$1/k_d(\theta, T)$
τ_{eff}	characteristic time for effusion from the μKEC	s	$V/(FA_0)$
Dimensionless variables and parameters:			
c'	adsorbate concentration		$cV/A\sigma_0$
$S(\theta, T)$	coverage dependent adsorbate sticking coefficient		
S_0	sticking coefficient at $\theta = 0$		
δ	sample area to orifice area ratio		A/A_0
θ	fractional adsorbate surface density		σ/σ_0
Subscripts			
m	at desorption peak		
i	initial value		

where A is the area of the sample and τ_{des} and τ_{ads} are characteristic times associated with τ_{des} and r_{ads}. These and all other terms are defined in table 1. The rate of effusion from the cell can be expressed as

$$r_{eff} = \frac{c'}{\tau_{eff}} = \frac{FA_0}{A\sigma_0 RT} P = \frac{FA_0}{V} c', \tag{5}$$

where A_0 is the area of an ideal orifice with the same conductance as the outlet port or pumping port of the sample chamber, and τ_{eff} is a characteristic time associated with r_{eff}. Although we have specified effusion as the method of removing adsorbate molecules from the μKEC, a similar pumping effect would be produced by flowing inert gas through the cell. During a thermal desorption

experiment, a signal proportional to r_{eff} is measured along with the sample and cell temperature.

The accumulation term, dc'/dt, in eq. (2) can be set to zero by assuming a quasi-steady state condition [12] exists in the gas phase. The quasi-steady state assumption is valid only if the characteristic response time of the gas phase is significantly faster than that of the surface phase. The criterion for quasi-steady state in the gas phase is usually easy to meet experimentally and can be expressed for this model as

$$\frac{\tau_{\text{ads}}/\tau_{\text{des}}}{1+[\delta S(\theta,T)]^{-1}} = \frac{V\delta}{AF}\left(\frac{\nu_0 \exp(-E_{\text{d}}/RT)}{1+\delta S_0(1-\theta)}\right) \ll 1, \tag{6}$$

where δ is the ratio of the sample area A to the equivalent outlet orifice area A_0. The parameter δ is the key design parameter for the Micro Knudsen Effusion Cell technique: operation at high δ, that is, a high ratio of sample surface area to pumping speed, allows thermal desorption at relatively high pressure, as shown below.

With dc'/dt set to zero, eq. (2) can be used to show that r_{des}, r_{ads}, and r_{eff} are related by a function of $\delta S_0(1-\theta)$. Expressing r_{ads} in terms of r_{des}, eq. (1) can be rewritten as

$$\frac{d\theta}{dt} = -r_{\text{des}}\left(\frac{1}{1+\delta S_0(1-\theta)}\right) = -\nu_0 \exp\left(\frac{-E_{\text{d}}}{RT}\right)\left(\frac{\theta}{1+\delta S_0(1-\theta)}\right). \tag{7}$$

For a linear temperature ramp, $T = T_{\text{i}} + \beta t$, Cvetanovic and Amenomiya [10] solved an equivalent set of equations only for the limiting cases (a) $\delta \to 0$, their "readsorption does not occur" case corresponding to desorption into UHV, and (b) $\delta \to \infty$, their "readsorption occurs freely" case corresponding to desorption at relatively high adsorbate pressures where adsorption–desorption equilibrium is closely approached. Following a solution procedure similar to Cvetanovic and Amenomiya's, we have developed a general solution for eq. (7) that is valid over all values of δ. At the desorption peak, parameters can be related by

$$\frac{E_{\text{d}}}{RT_{\text{m}}} = \ln\left(\frac{\nu_0}{\beta}\right) + \ln\left(\frac{T_{\text{m}}[1+\delta S_0(1-\theta_{\text{m}})]^2}{(E_{\text{d}}/RT_{\text{m}})(1+\delta S_0)}\right), \tag{8}$$

$$P_{\text{m}} = \delta\beta\sigma_0\theta_{\text{m}}\left(\frac{2\pi MR}{T_{\text{m}}}\right)^{1/2}\left(\frac{E_{\text{d}}}{RT_{\text{m}}}\right)\left(1-\frac{\theta_{\text{m}}}{1+(\delta S_0)^{-1}}\right), \tag{9}$$

where T_{m}, P_{m}, and θ_{m} are the temperature, pressure, and fractional adsorbate surface density, respectively, at the measured "desorption peak" maximum in P, $-d\theta/dt$, and r_{eff}. The fact that $\theta_{\text{m}} \approx 0.37\ \theta_{\text{i}}$ over a wide range of parameters can be used to further simplify eqs. (8) and (9). Application of the μKEC technique is not limited to the simple adsorption and desorption kinetics and

the linear temperature ramp considered in this model. However, the analytical solution of this simple model does allow one to assess the relationships between the experimental design parameters and the system variables relatively easily.

Eqs. (8) and (9) allow one to calculate two unspecified or unknown parameters and can be used as analysis tools and as design tools along with eq. (6). For example, for the case of desorption into UHV with high pumping speed ($\delta \rightarrow 0$), it has been common practice in the literature [11] to assume a value of ν_0 in order to estimate E_d, using a T_m determined at the maximum in a measured signal proportional to P or r_{eff}. However, eqs. (8) and (9) show that both ν_0 and E_d can be determined when P_m and θ_m are determined as well as T_m. For an adsorbate–adsorbent system about which some information is known, β and δ can be chosen in the design of experiments in order to obtain measurements over a desired range of temperature and pressure.

Eq. (9) shows that the adsorbate pressure over a sample increases as the parameter δ is increased. That is, thermal desorption can be performed under relatively high pressures for high ratios of sample area to pumping speed. Although not as immediately apparent, eqs. (7)–(9) also demonstrate that the temperature at which a given coverage is established increases as δ increases.

As δ is increased, V must be decreased in order to satisfy the criterion for quasi-steady state in the gas phase, eq. (6). For low surface area samples, thermal desorption can be done by enclosing the sample in a "micro UHV chamber" or cell with a small pumping port. A mass spectrometer located external to the cell can be used to measure $r_{eff}(t)$. $P(t)$ can be determined from r_{eff} knowing the cell temperature and conductance of the pumping port. From integration of r_{eff} over time, $\theta(t)$ can be determined.

Fortunately, and perhaps surprisingly, increasing δ by decreasing the conductance of the pumping port does not significantly reduce the instantaneous effusion rate $r_{eff}(t)$ to be detected by the mass spectrometer. This is because the increase in pressure inside the sample cell compensates for the decrease in conductance, although a small decrease in instantaneous effusion rate will occur due to broadening of desorption peaks as δ is increased.

Table 2 presents a comparison of five cases in which design parameters are varied for a hypothetical adsorbate–adsorbent system that approximates the CO–Pt system. Case A represents thermal desorption from a single crystal at high pumping speed ($\delta \rightarrow 0$), or "into UHV", at 1 K/s. Case B represents thermal desorption from a single crystal in a μKEC at 1 K/s that results in a peak desorption pressure in the pressure gap. Comparing case B to case A, P_m has increased approximately three decades and T_m has increased by about 30 K. Case C represents thermal desorption from a single crystal into UHV at 100 K/s. Increasing β produces a higher P_m and T_m than case A, but fails to produce a P_m equivalent to that of case B. Increasing δ in a μKEC has an effect similar to but much stronger than that of increasing β in UHV thermal desorption.

Table 2
Comparison of cases for which δ and β are varied for a hypothetical adsorbate–adsorbent system described by eqs. (1)–(9) and approximating the CO–Pt system. Constant parameters are: $\nu_0 = 10^{14}$ s^{-1}, $S_0 = 0.5$, $\sigma_0 = 2.5 \times 10^{-5}$ mol/m^2, $\theta_i = 1.0$ at $T_i = 295$ K, $E_d = 100$ kJ/mol, $V = 0.14$ cm^3

Case	A (cm^2)	A_0 (cm^2)	δ	β (K/s)	T_m (K)	θ_m	P_m (Pa)	V_{max} (cm^3)	r_{ads}/r_{des} (at peak max.)
A	1	10	0.1	1	348	0.39	2.1×10^{-6}	1300	0.029
B	1	0.01	100	1	380	0.36	1.1×10^{-3}	2.5	0.97
C	1	10	0.1	100	398	0.39	1.8×10^{-4}	18	0.029
D	100	10	10	1	358	0.39	1.4×10^{-4}	2100	0.021
E	100	0.01	10000	1	439	0.36	9.1×10^{-2}	3.6	0.9997

Cases D and E represent μKEC thermal desorption from a porous catalyst sample consisting of 10 mg of 1 wt%-Pt/Al_2O_3 at 100% dispersion. The sample could be spread over an area of 1 cm^2 to produce layer with a thickness of 100 μm. With such a thin layer, the problems presented by having strong diffusional gradients in a porous catalyst would be significantly reduced [13]. Gorte [14] analyzed this problem and provided a set of criteria to determine the extent of diffusional gradients in a porous catalyst layer. With the additional area provided by the catalyst sample and small δ, case E has a large P_m and a high T_m. If a 0.1 mg sample was used, the surface area of 1 cm^2 would provide a mass spectrometer signal similar to that of 1 cm^2 single crystal. If spread over 1 cm^2, the layer thickness would be only 1 μm and would have negligible diffusional resistance across the sample layer.

The P_m values for cases B and D are separated by only a decade. The μKEC method of thermal desorption provides a means to obtain kinetic and thermodynamic parameters for both well-characterized single crystals and high-surface-area porous catalysts at similar conditions of adsorbate pressure and temperature.

The ultimate value for P_m is limited by the surface area one is able to place in a sample cell. Use of porous catalysts provides the most surface area but is restricted by the requirement to avoid diffusional gradients. Diffusional gradients can be reduced by reducing $r_{eff} = r_{des} - r_{ads}$, the net rate of desorption from the sample. By increasing δ (reducing A_0), r_{eff} is reduced and a higher P_m obtained. This higher P_m will reduce concentration gradients and allow more surface area to be put in the μKEC. This synergistic effect continues as δ is increased until a diffusional gradient constraint is violated or no more sample can be put into a cell volume that satisfies eq. (6). Table 2 gives the maximum allowable cell volume, V_{max}, corresponding to a volume that would make the left hand side of the eq. (6) equal to 0.001.

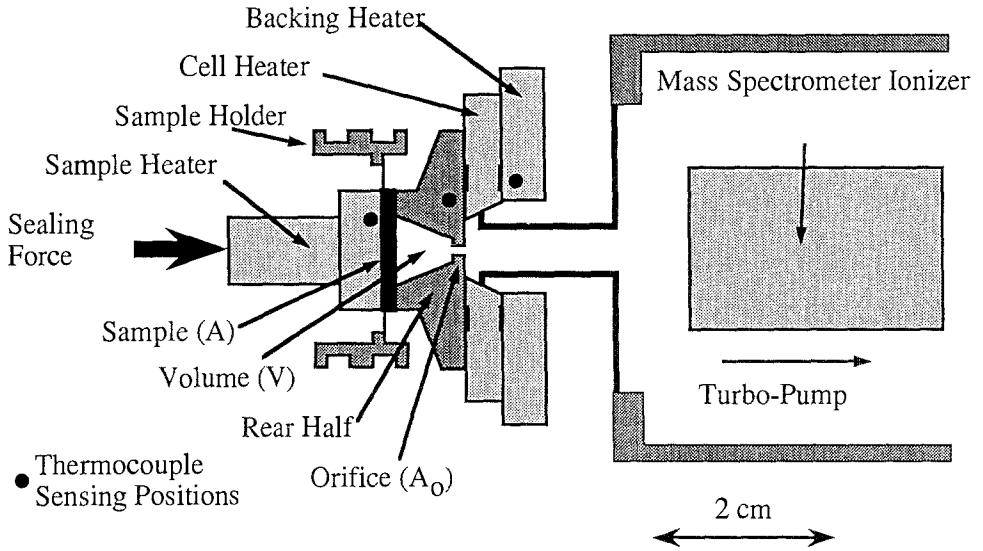

Fig. 1. Experimental apparatus for performing Micro Knudsen Effusion Cell (μKEC) thermal desorption (schematic cross section). The entire assembly is enclosed in a surrounding UHV chamber. Thermocouples are used to maintain the temperatures of the sample and μKEC rear half the same during the temperature ramp. Adsorbate molecules that desorb from the sample can readsorb onto the sample or effuse through a small orifice and be detected by the differentially pumped mass spectrometer.

The degree of approach to adsorption–desorption equilibrium for the cases considered is also given in table 2. As $\delta \to 0$, $r_{ads}/r_{des} \to 0$ and experimental results will contain information about the desorption process only. As $\delta \to \infty$, $r_{ads}/r_{des} \to 1$ and experimental data will contain information about the ratio between adsorption and desorption rates, that is, about adsorption–desorption equilibrium only. Experiments performed over a range of δ, especially at the extreme limits, would allow determination of both adsorption and desorption rate parameters. Alternatively, adsorption rate measurements could be used in conjunction with μKEC experiments at large δ to determine adsorption and desorption rate parameters separately.

3. Micro Knudsen Effusion Cell (μKEC) apparatus

A schematic cross section of the μKEC apparatus we have built is shown in fig. 1. The assembly shown is enclosed in a surrounding main UHV chamber. This main UHV chamber is also connected to a pretreatment chamber and an XPS system. Samples are mounted on modified Perkin-Elmer PHI sample holders. In fig. 1, a sample is shown sealed against the cell's rear half. Samples

can be retracted from this sealed position and moved in UHV to a position in front of a dosing head in the main UHV chamber and to positions in the pretreatment chamber and the XPS system with the use of manipulators. When a sample is sealed against the rear half of the μKEC as shown in fig. 1, an area A (0.46 cm^3) of the sample is exposed to the inside of the cell and a small chamber of volume V (0.14 cm^3) is performed by the face of the sample and the cell's rear half. During a thermal desorption experiment, gas-phase adsorbate molecules can readsorb on the sample or escape from the cell by effusion through a pumping port (0.1 cm diameter by 0.15 cm) with a conductance (42 cm^3/s at 300 K) equivalent to that of an ideal orifice of area $A_0 = 0.0036$ cm^2. The value of δ corresponding to this sample area and orifice area is 130. Molecules effusing through the pumping port enter the mass spectrometer chamber where the effusion rate is measured.

A turbo-pump maintains UHV in the mass spectrometer chamber such that back-streaming from the mass spectrometer chamber into the sample cell is negligible. Except for the cell's pumping port, the mass spectrometer chamber is isolated from the main UHV. The quadrupole mass spectrometer is computer controlled so that multiple mass peaks can be read during an experiment. The mass spectrometer was calibrated to relate its signal quantitatively to the rate of effusion, r_{eff}. This was done by recording the mass spectrometer signal and pressure in the main UHV chamber at steady state (a) with a known leak rate of CO into the main UHV chamber from a manifold-capacitance-manometer system of known volume and (b) with the sample holder retracted such that the main UHV chamber was pumped only by the effusion cell's pumping port. Measurements were made in order to correct for pumping by the ionization gauge in the main UHV chamber and by small leaks between the main UHV chamber and the mass spectrometer chamber other than the cell's pumping port. The calibration measurements also provided the pumping port conductance, which agreed with the theoretically calculated conductance.

The walls of a μKEC should be inert with regard to adsorption and desorption and should not contaminate samples. For our initial system, CO/Pt, we chose OFHC Cu as the wall material because CO adsorption over Cu is weak [15,16] relative to CO adsorption over Pt. As we discuss below, surface coverages of CO over Cu are extremely low in the pressure and temperature ranges covered by our experiments. XPS analysis of the surface and the reproducibility of thermal desorption experiments show that neither Cu nor other impurities contaminate the sample. For other adsorbate–adsorbent combinations, a different wall material may be required. For example, use of sapphire, clad by a heater, should be inert for many applications, provide reversible seals to the sample, and provide for introduction of optical probes for spectroscopic analysis during desorption or reaction. Some sticking of the Cu and Pt, presumably by diffusion bonding, was observed after many open–close cycles and this problem should also be avoided with the use of a cell material such as sapphire.

A force applied to the sample heater seals the sample against the cell's rear half and ensures adequate thermal contact between the sample heater, sample, and the cell's rear half. A separate heater (OFHC block with embedded insulated resistance wires) heats the cell's rear half. Thermocouples embedded in the sample heater and the cell are used for feedback control to keep the two temperatures the same (usually within ± 1 K) as their temperatures are ramped during an experiment. Adsorbate molecules striking the sample have the same temperature as the sample. This "hot wall" feature of the μKEC is unique. In other "pressure gap" adsorption–desorption experiments, such as laser-induced thermal desorption [17] or low-energy molecular beam scattering [18], the average temperature and temperature distribution of incoming adsorbate molecules is markedly different than that of the sample.

Dosing of samples can be performed using a dosing head in the mean UHV chamber or by back-filling the mass spectrometer chamber while the sample is sealed against the cell. Using isotopically labeled CO, we determined that only a negligible amount of the CO detected during a desorption run desorbed from surfaces other than the sample.

The apparatus shown in fig. 1 was used to perform thermal desorption of CO from a polycrystalline Pt foil (0.1 mm thick 99.998%, Johnson–Matthey). Since this project is in a developmental stage, a low-cost Pt foil was used rather than a single crystal, although the technique is directly applicable to single crystals. The foil was cleaned by a sequence of heating at temperatures up to 773 K, in vacuum, 100 Pa H_2 and 100 Pa O_2. Finally, Ar-ion sputter cleaning was performed until XPS spectra showed no further reduction in surface carbon contamination. The surface carbon contamination was determined to be less than one-third of a monolayer using angle-resolved XPS depth profiling [19]. The main requirement for this developmental stage of the work is that the surface have constant characteristics and give reproducible desorption spectra. The foil used gave reproducible desorption spectra in the course of over 30 adsorption–desorption cycles. In future work, the technique can be used to obtain fundamental information about well-defined single crystal surfaces.

Fig. 2 shows the results of one of a series of thermal desorption experiments that were conducted at various heating rates and starting adsorbate coverages [6]. For this experiment, the sample was dosed to saturation with CO at room temperature by back-filling the mass spectrometer chamber while the sample was sealed against the cell, followed by pumping out the cell and mass spectrometer chamber. The run was started at a room temperature and a smoothly varying nonlinear temperature ramp, 0.7 K/s at 350 K and 4.4 K/s at 555 K, was performed. Although the model equations above were solved for a linear temperature ramp, a linear ramp is not a requirement for quantitative analysis of data. The CO pressure inside the cell over the Pt was determined using the cell temperature and the mass flux calibration of the mass spectrometer. The adsorbed CO surface density, $\theta(t)$, was determined by integrating the mass

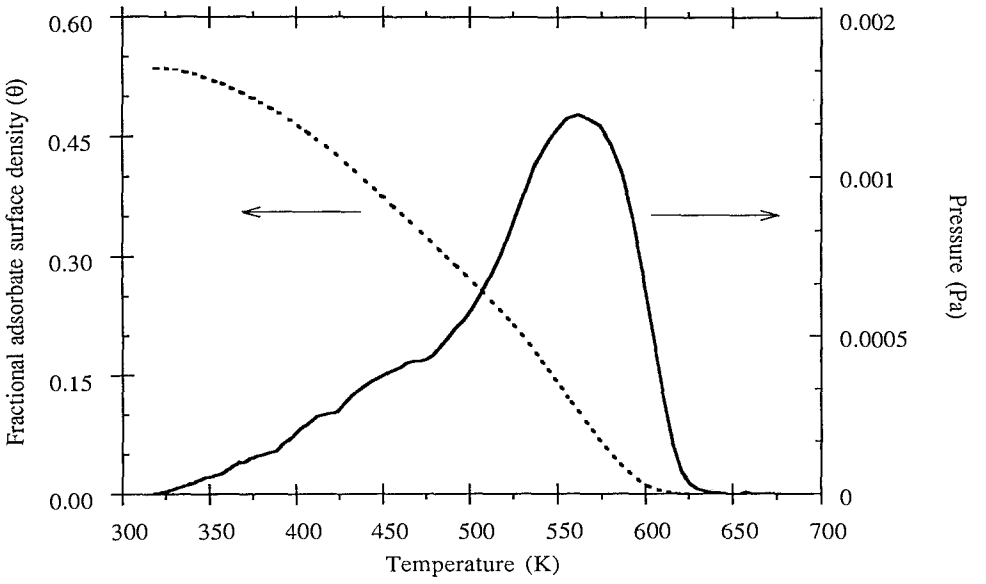

Fig. 2. Fractional CO surface density (θ) and CO pressure at near-equilibrium over a polycrystalline Pt foil for a μKEC thermal desorption experiment.

spectrometer signal for the entire desorption run. The value determined for θ_i, 0.54, (using $\sigma_0 = 2.5 \times 10^{-9}$ mol/cm^2) is in close agreement with values reported for clean Pt surfaces exposed to tens-of-Langmuirs of CO, and the desorption curve is similar in shape to those reported for CO desorption from polycrystalline Pt foils [20]. Under the conditions of this experiment, $r_{ads}/r_{des} \rightarrow 1$ and the P, T, θ values shown in the figure represent near-equilibrium values.

Using the coverage-dependent sticking coefficients and desorption rate parameters for CO over Cu(110) obtained by Harendt et al. [15], we took the measured pressures in fig. 2 and estimated the equilibrium CO coverages present on the Cu walls of the sample cell during the experiment. At all times during the experiment, we estimate that the fractional coverage of CO on the Cu is less than 1×10^{-6} and that the fraction of CO molecules adsorbed on the 1.1 cm^2 of Cu relative to those adsorbed on the 0.46 cm^2 of Pt was less than 5×10^{-6}, confirming that the Cu walls can be considered inert with respect to CO adsorption under our experimental conditions.

A peak CO pressure of 1.2×10^{-3} Pa was obtained over the sample during the experiment shown in fig. 2, well into the pressure gap. This peak pressure was obtained with the relatively large pumping port shown in fig. 1. Significantly higher pressures can be obtained with smaller pumping ports. Experiments performed at relatively high pressures in the μKEC provide for close approach to thermal and adsorption equilibrium conditions and can be used to verify separate measurements of adsorption and desorption rates in UHV. Also, the establishment of a given surface coverage under relatively high pressure and,

thus, temperature in the μKEC can provide a check on whether side reactions occur at higher temperatures than those established at the same coverage during thermal desorption in UHV.

Acknowledgement

Support for this project was provided by the National Science Foundation under Grant Number CBT-8715427. KG is a Ford Foundation and University of California President's Dissertation Fellow.

References

[1] J.L. Falconer and J.A. Schwarz, Catal. Rev.-Sci. Eng. 25 (1983) 141.
[2] D.A. King, Surf. Sci. 47 (1975) 384.
[3] J.L. Falconer and R.J. Madix, J. Catal. 48 (1977) 262.
[4] J.L. Taylor and W.H. Weinberg, Surf. Sci. 78 (1978) 259.
[5] K.V. Guinn and R.K. Herz, Direct Comparison of Thermal Desorption from Supported Metal and Metal Single Crystal Catalysts, presented to Am. Inst. Chem. Eng., Chicago, IL, November 11–16, 1990.
[6] K.V. Guinn, Ph.D. Dissertation, University of California, San Diego (1991).
[7] G.A. Somorjai, Surf. Sci. 89 (1979) 496.
[8] M.J. Mummey and L.D. Schmidt, Surf. Sci. 109 (1981) 43.
[9] M. Ungarish and L.D. Schmidt, Appl. Surf. Sci. 17 (1983) 23.
[10] R.J. Cvetanovic and Y. Amenomiya, Advan. Catal. 17 (1967) 103.
[11] P.A. Redhead, Vacuum 12 (1962) 203.
[12] J.R. Bowen, A. Acrivos and A.K. Oppenheim, Chem. Eng. Sci. 18 (1963) 177.
[13] R.K. Herz, J.B. Kiela and S.P. Marin, J. Catal. 73 (1982) 66.
[14] R.J. Gorte, J. Catal. 75 (1982) 164.
[15] C. Harendt, J. Goschnick and W. Hirschwald, Surf. Sci. 152/153 (1985) 453.
[16] L.D. Peterson and S.D. Kevan, Surf. Sci. Lett. 235 (1990) L285.
[17] E.G. Seebauer, A.C.F. Kong and L.D. Schmidt, Surf. Sci. 176 (1986) 134.
[18] C.T. Campbell, G. Ertl, H. Kuipers and J. Segner, Surf. Sci. 107 (1981) 220.
[19] V.I. Nefedov, transl. by N.G. Shartse, *X-ray Photoelectron Spectroscopy of Solid Surfaces*, 1st Engl. Ed. (VSP, Utrecht, 1988).
[20] M.A. Morris, M. Bowker and D.A. King, in: *Comprehensive Chemical Kinetics. Vol. 19. Simple Processes at the Gas–Solid Interface*, eds. C.H. Bamford, C.F.H. Tipper and R.G. Compton (Elsevier, Amsterdam, 1984) p. 47.